#2434

AIVC 1904

2434

The flow resistance of experimental models of naturally occurring cracks

G C Gardner, BSc, DSc(Eng) and **R J Tyrrell**, BSc
Central Electricity Research Laboratories, Leatherhead, Surrey

Naturally occurring cracks have rough surfaces which mate in such a fashion as to close the crack completely when the surfaces are pressed together. Experimental work shows that friction factors are given by a Nikuradse type of equation when the crack surfaces are widely spaced. The equation remains applicable as the crack closes until roughness elements from opposing surfaces start to overlap and then an upper limit is achieved. Further reduction in the crack wall separation causes a reduction in the friction factor, which may fall to the level applicable to a smooth-walled tortuous channel. These observations are in accord with theoretical concepts.

NOTATION

a	dimensionless wave amplitude
A	surface area per unit projected area
d	packing element size in packed bed
d_s	sand grain size
f	friction factor, equation (3)
h	roughness height
n	constant
s	distance over surface
S	distance over surface per unit projected distance
v	velocity in x direction
w	crack wall separation
x	rectilinear distance through crack in flow direction ignoring roughness
x_0	wavelength
y	distance normal to x direction and in direction of crack separation
$\frac{dp}{dx}$	pressure gradient
Re	crack Reynolds number, equation (2)
Re_p	packed-bed Reynolds number, equation (8)
Δ	root mean square surface elevation from mean elevation
ε	packed-bed voidage
θ	angle of true flow direction to x direction
ν	kinematic viscosity
ρ	density
ϕ	packing element shape factor
ψ	packed-bed friction factor, equation (8)

1 INTRODUCTION

Naturally occurring cracks have two opposing rough surfaces which will mate and seal completely if they are pressed together, and it may be necessary to know the crack's resistance to flow when it occurs undesirably in a barrier wall between fluids at different pressures. An example of present interest to the writers is of the tubing containing water circulated from the reactor core of a PWR. It passes through the steam generator with a 90 bar pressure differential over the tube wall. If a stress corrosion crack forms, the rate of leakage can be measured by the rate of build-up of radioactivity on the low-pressure side and it is then required to relate this rate to the size of the crack. The crack wall separation may be less than 20 μm while the metal grains, which afford roughness, may have a size which is also 20 μm.

If crack walls are separated by a large distance compared to the size of the roughness elements, the manner in which the friction factor for turbulent flow will vary with wall separation is well known and is based upon the classic work of Nikuradse (1) with pipes whose walls were coated with sand. Recently, Button *et al.* (2) have given confirmation with cracks composed of plane grit-blasted walls and much other confirmation is available in the literature.

When the wall separation is reduced it is necessary to know when and how the Nikuradse approach will break down. This has been answered to a limited extent in the literature by those who have sought to define the location of the wall when applying Nikuradse's equations. It was not of importance to Nikuradse, whose largest sand grain was a thirtieth of the pipe diameter, but reasonably the location should lie between the bottom and top of the roughness elements. Bayazit (3) reviewed experimental information which places the effective wall at 0.15–0.3 times the diameter of both spherical and hemispherical roughness elements below the tops of the elements projecting into the stream. His own work gave a coefficient of 0.35 but none of this may be applicable here, where a projection from one wall corresponds to a geometrically similar cavity on the other wall. The consequent direction of the flow by the roughness could utilize the available flow volume more effectively than without the correlation of roughness on the two walls.

The manner in which the Nikuradse approach breaks down is the chief interest of the present work. It will be argued in the next section that, at least when the roughness elements from opposing walls start to overlap, the system may start to resemble a packed bed rather than two plane rough walls. MacDonald *et al.* (4) have critically reviewed the information on pressure drop through packed beds and recommend the Ergun (5) equation with slightly modified numerical coefficients. This will be shown to suggest that the friction factor is independent of the wall separation. Therefore, it may be expected that the rise in the friction factor, according to

The MS was received on 16 August 1985 and was accepted for publication on 2 January 1986.

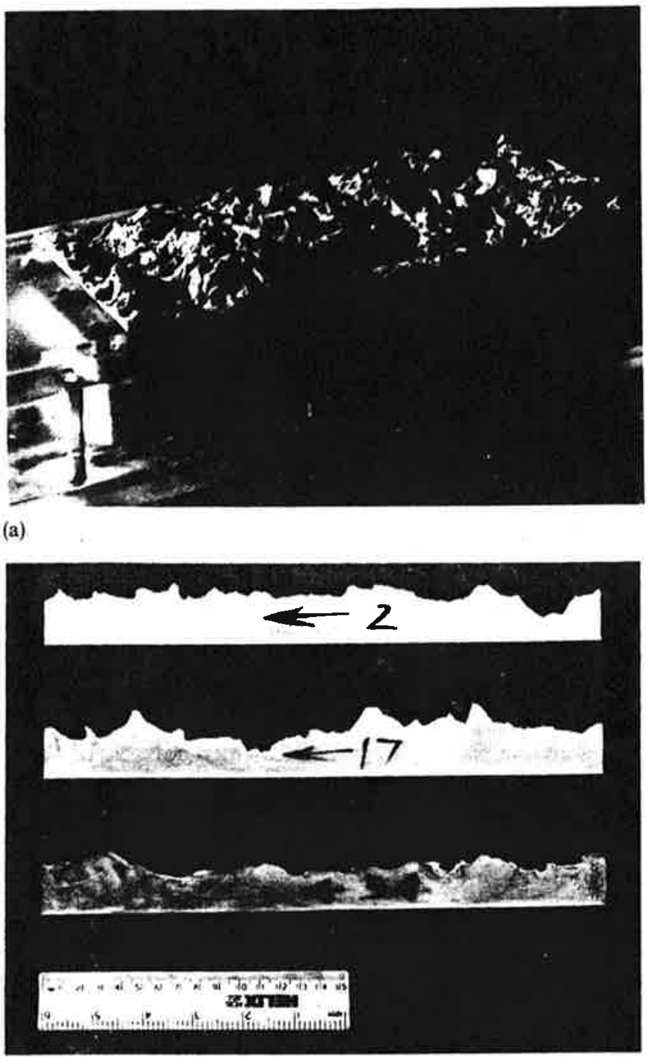

(a)

(b) **Fig. 1** The aggregate crack
(a) Lower crack surface.
(b) Slices from the epoxy cast.

Nikuradse, as the separation is reduced will be halted. However, this is not the end of the matter, not only because the Ergun equation has not been tested for very low packed-bed voidages but also because one can visualize that, with very small separations, the system may start to resemble a smooth-walled but tortuous flow channel. It is therefore not impossible that once the friction factor has reached an upper limit, as seen through the Ergun equation, it may fall as the wall separation decreases further.

These conjectures will be put in quanitative form in the next section and then experiments will be described and discussed. Two types of surface with the required characteristics were tested, and they are shown in the photographs of Figs 1 and 2. Figure 1 is from what will be called the aggregate crack, because it was made by fracturing an aggregate of granite chips set in plaster of Paris. The surface of Fig. 2 is much more artificial and is a wall of what will be called the giant's causeway crack. The reason for this name will become apparent later. Here it needs only be noted that the opposing wall had the important characteristics that it was identical geometrically to the other. The two walls of the aggregate crack were identical in a more random fashion.

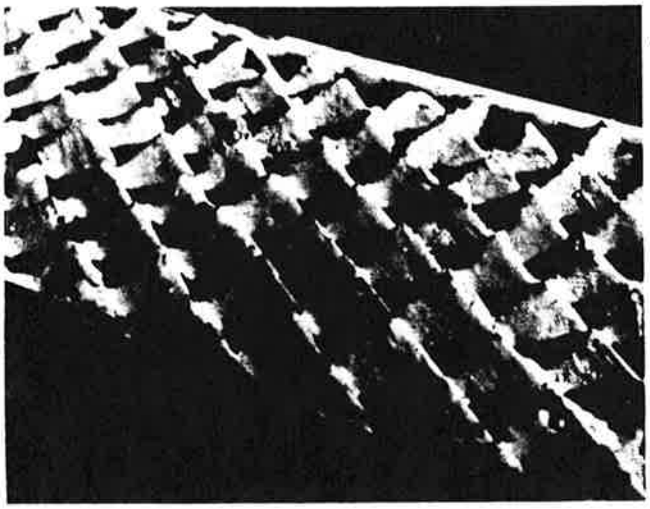

Fig. 2 Surface of the giant's causeway crack

2 THEORY

2.1 Large crack wall separation

First consider smooth crack walls. For laminar flow the friction factor is given by

$$f = \frac{24}{Re} \tag{1}$$

where

$$Re = \frac{2vw}{\nu} \tag{2}$$

where v is the average velocity, w is the wall separation and ν is the kinematic viscosity. The friction factor is defined by

$$f = \frac{w(\mathrm{d}p/\mathrm{d}x)}{\rho v^2} \tag{3}$$

where $\mathrm{d}p/\mathrm{d}x$ is the pressure gradient and ρ is the density.

For turbulent conditions the Blasius equation (6) is

$$f = 0.079(Re)^{-0.25} \tag{4}$$

The treatment of sand roughness is given in Schlichting (6). Only the result for a fully turbulent condition will be required and the analysis for a pipe has been adapted to the case of flow between parallel walls. The result is

$$\frac{1}{f} = 3.125\left[\ln\left(\frac{5.5w}{d_s}\right)\right]^2 \tag{5}$$

where d_s is the sand grain size.

Equations (1), (4) and (5) are plotted in Fig. 3.

It may be noted that Button *et al.* (2) measured the resistance of cracks with grit-blasted walls and with w varying between 0.1 and 1.0 mm to the flow of nitrogen. They measured the root mean deviation of the surface elevation, Δ, from the mean elevation with a surface profilemeter and w/Δ was varied in their experiments from 10 to 500. They expressed their results by

$$\frac{1}{f} = 3.82\left[\ln\left(\frac{w}{1.8\Delta}\right)\right]^2 \tag{6}$$

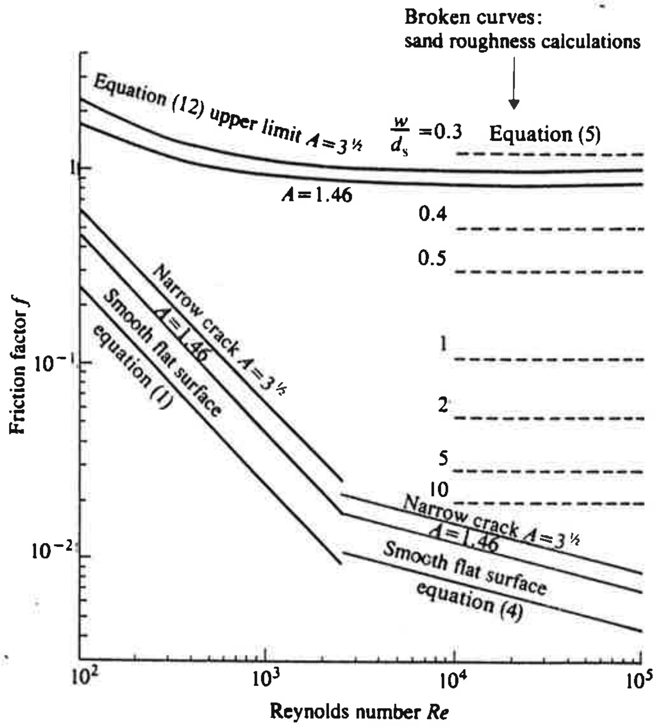

Fig. 3 Laminar and turbulent flow regimes: upper and lower limits to the friction factor

Comparison of equations (5) and (6) suggests that d_s/Δ lay between 5.5 and 8.3. The roughness height h was greater than Δ by an unknown factor. It is also of interest that Pfau (7) examined available data on hydraulic resistance of naturally occurring ripples, such as ripple magnetite in boiler tubes. They give high friction factors for given roughness heights h, and Pfau found that d_s/h varied from 2.6 to 8.9 with an average of 4.8.

2.2 A possible upper limit to the friction factor

The Ergun equation with the modified numerical coefficients suggested by MacDonald *et al.* (4) is

$$\psi = \frac{40}{Re_p} + 0.6 \tag{7}$$

where

$$\psi = \frac{2(dp/dx)}{\rho v^2} \frac{\varepsilon d}{\phi(1-\varepsilon)}$$
$$Re_p = \frac{4v}{\nu} \frac{\varepsilon d}{\phi(1-\varepsilon)} \tag{8}$$

where d is the packing element size, ε is the voidage and ϕ is the shape factor, which is defined as the surface area of the packing element divided by its volume and multiplied by d. Thus $\phi = 6$ for a sphere.

A model of the crack is considered in which packing elements project a distance nd through a plane wall, where n is a numerical coefficient. When the crack is closed, the equivalent packed bed therefore has a width of nd. When the crack is opened a distance w, the voidage is

$$\varepsilon = \frac{w}{nd + w} \tag{9}$$

and

$$\frac{\varepsilon d}{1-\varepsilon} = \frac{w}{n} \tag{10}$$

Since the crack closes completely to leave no voidage, the volume of packing elements per unit project surface area of the crack wall is nd. Let A be the actual surface area of a crack wall per unit projected area. From the definition of ϕ we have $\phi = 2A/n$. Thus, using the definition of f and Re given by equations (2) and (3) equation (8) transforms to

$$\psi = \frac{f}{A}$$
$$Re_p = \frac{Re}{A} \tag{11}$$

and equation (7) becomes

$$f = \frac{40A^2}{Re} + 0.6A \tag{12}$$

The Appendix shows that A for the giant's causeway is calculated to be $3^{1/2}$. The measurement of A for the aggregate crack will be described later. It is 1.46. Equation (12) with these two values of A is plotted in Fig. 3.

2.3 A possible lower limit to the friction factor as the crack wall separation becomes very small

When the crack wall separation is small compared to the size of the roughness elements the system is one of flow in a tortuous passage. To estimate a lower limit to the friction factor, which may occur when the separation is less than that to obtain the upper limit described in Section 2.2, it will be assumed that the passage walls are smooth and that there are no form drag losses.

A simple model is conceived of a two-dimensional passage in the x–y plane with the x direction being the general forward direction, in which the velocity is v. The passage walls are a constant distance w apart in the y direction and, locally, are at an angle θ to the x direction. The velocity in the passage is, therefore, $v \sec\theta$ and the passage width normal to this velocity is $w\cos\theta$. The distance moved along the passage for a differential distance dx is ds = d$x \sec\theta$. Now, for viscous flow, the pressure gradient is proportional to the average velocity divided by the square of the channel width, and it is deduced that the pressure gradient in the x direction is proportional to $\sec^4\theta$. In turbulent flow the pressure gradient is proportional to the friction factor times the square of the velocity and divided by the channel width. However, the friction factor is a function of the Reynolds number, which is independent of θ and, again, it is deduced that the pressure gradient is proportional to $\sec^4\theta$.

Consideration must now be given to tortuosity normal to the x–y plane. Let S be the distance along the surface in the x–y plane divided by the projected distance and assume that this parameter is applicable normal to the x–y plane. Clearly all velocities must be divided by S. Thus, in viscous flow there is a correction factor $\sec^4\theta/S$ and in turbulent flow $\sec^4\theta/S^{1.75}$. The exponent of 1.75 instead of 2 is used to make allowance for the variation of the friction factor with the velocity, as given by equation (4).

The simple assumption is made that the passage walls in the x–y plane are represented by a sine wave

$$\frac{y}{x_0} = a \sin\left(2\pi \frac{x}{x_0}\right) \tag{13}$$

where x_0 is the wavelength and a is the dimensionless amplitude. S can be calculated as a function of a by integration of equation (13). It is also assumed that $S = A^{1/2}$. $S = 1.21$ for the aggregate crack, which, therefore, has $a = 0.157$ for the equivalent sine wave, and $S = 1.32$ for the giant's causeway crack, so that $a = 0.198$.

Finally, the average value of $\sec^4 \theta$ can be determined by numerical integration using equation (13), and the multiplying factors for the straight channel friction factors can be obtained to be applied to equations (1) and (4). For the aggregate crack these factors are 1.93 for viscous flow and 1.67 for turbulent flow. The corresponding factors for the giant's causeway crack are 2.62 and 2.13. All these estimates are illustrated in Fig. 3.

3 EXPERIMENTAL APPARATUS AND METHOD

Fatigue or stress corrosion cracks may typically have a wall separation of 20 μm with a roughness element corresponding to metal grains of about the same size. In the PWR, the pressure differential over the steam generator tube walls is 90 bar. It is experimentally convenient for the manufacture of surfaces in the present work to scale-up by a factor of about 1000, and this has the additional advantage that the appropriate Reynolds numbers may be obtained with greatly reduced pressure differentials.

To manufacture the aggregate crack a cylindrical cast was made with nominally 19 mm granite chips set in plaster of Paris. A proportion of smaller chips was added to obtain a maximum concentration of granite. The cast was pressed between plane parallel walls to make line contact parallel to the axis of the cylinder. It fractured along an approximately plane surface without fracturing the aggregate itself.

One fracture surface was chosen and an epoxy resin cast was taken from it. This was machined to give a rectangular area of 290 mm in the flow direction and 120 mm in the other direction of the original rough surface surrounded by flat areas. A silicone rubber cast was taken of the rough area and this was placed in a Perspex channel, as shown in the photograph of Fig. 1 and the cross-section of the test section shown in Fig. 4. Figure 4 also shows the epoxy resin cast forming the upper wall of the crack and Perspex side walls of suitable height providing the crack separation.

There were three rows of three pressure tappings in the top crack wall and these were connected to water or mercury manometers, depending upon the magnitude of the pressures to be measured. Measurements of sets of three tappings transverse to the flow were averaged and used to obtain pressure drops for upstream and downstream lengths of the crack. When the crack was set up, depth gauges with modified probe heads were passed through the pressure tappings to check the crack separation.

The test section was studded to an upstream water supply box and was discharged to atmosphere. Water flowrates were measured by calibrated rotameters.

The surfaces for the giant's causeway crack were made from 50 mm lengths of 5 mm square fine-grained wood stock, as shown in Fig. 5. A first layer of stock, with corners meeting, was laid down in plasticine. A second layer was then glued in the angles of the first but with the ends set back 5 mm from the ends of the first layer. Third and subsequent layers were glued in place in a similar fashion. The surface including the ends of the stock comprised the required surface and in effect was an array of cubes with corners pointing out into the stream. If the glued assembly was stood with the axis of the 50 mm lengths of stock vertical, it resembled the geological curiosity known as the Giant's Causeway, which led to the naming of the crack. The crack was 150 mm in the flow direction and 44 mm in the other direction.

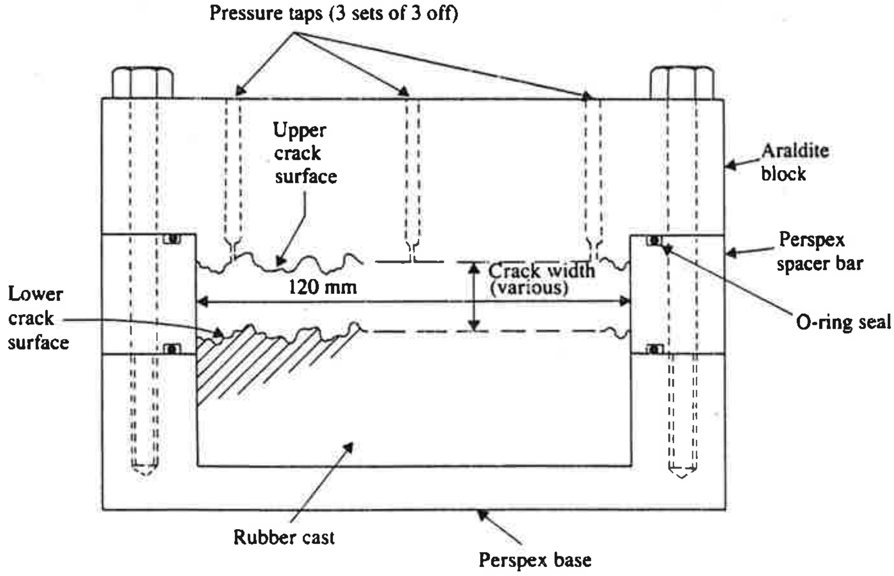

Fig. 4 Test section for the aggregate crack

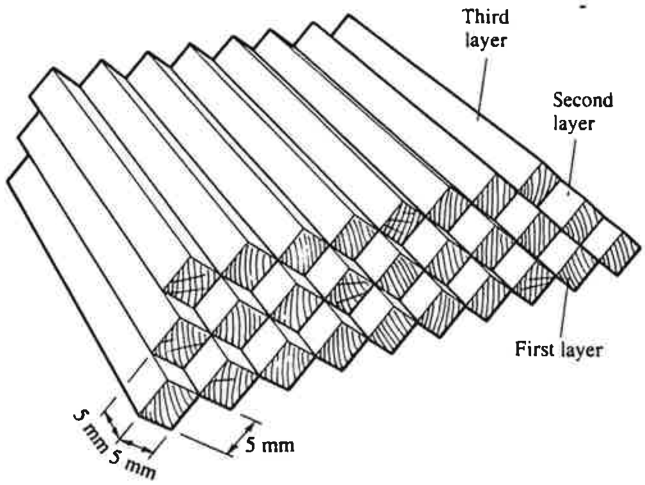

Fig. 5 Wooden pattern used to make the giant's causeway crack

An epoxy resin cast of the required surface of the glued assembly and a silicone rubber cast of that formed the experimental surfaces. The two surfaces were put into a test section similar to that for the aggregate crack but the upper crack surface of silicone rubber had an aluminium plate cast within it. Studs attached to this passed upwards through aluminium bracing bars joining the side walls of the test section and thumb screws on the studs then allowed the upper surface to be tightened down on brass bars which controlled the crack separation. Six pressure tappings at the centre-line in the flow direction passed through the upper wall to identical positions at the base of the roughness elements. Linear regression analysis of the pressure readings gave the pressure gradient.

When the giant's causeway crack wall separation was small and the water flowrate was small, rotameters could not be employed to measure the flowrate. A tall cylindrical Perspex vessel, which was open to the atmosphere, was then attached to the upstream water supply box. Water was drained from the vessel through the crack and the level was measured with respect to time. This gave the flowrate with respect to level so that setting a constant level by continuously supplying the vessel with water gave a required flowrate.

An additional epoxy resin cast of the aggregate surface was made and was cut into 34 slices, three of which are shown in Fig. 1. These were placed upon a digitizing table to obtain data for the calculation of the distance along the surface of the slice divided by the projected area of the slice. This ratio was found to be 1.21.

4 RESULTS AND DISCUSSION

Figure 6 gives the experimental results in terms of friction factor versus Reynolds number for the giant's causeway. The data for crack separation of 5.65, 6.31 and 9.55 mm agree with the Nikuradse-type equation (5) if $d_s = 2.9h$, where h is the height of the roughness element, which equals 5.77 mm. The multiplying factor is of the magnitude expected from other work such as that of Button *et al.* (2) and Pfau (7). Of greater interest is that it appears to be appropriate to assume that the wall starts from the bottom of the roughness elements.

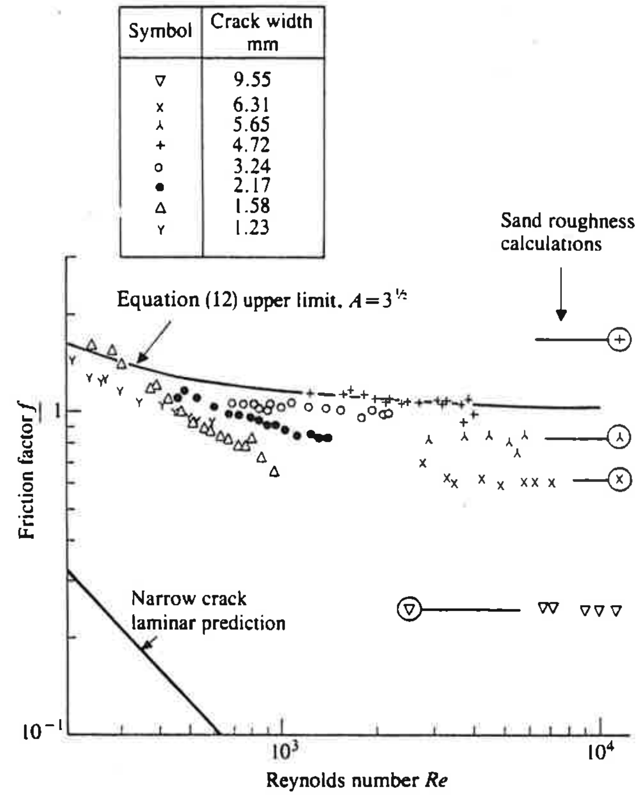

Fig. 6 Giant's causeway crack: friction factors versus Reynolds number

Figure 6 shows the estimates of the turbulent friction factor from equation (5) for the three crack separations noted above. The prediction for the next narrowest crack of 4.72 mm separation is 1.69, whereas the experimental value is 1.05. Clearly, the rise of the friction factor is limited and the limitation is seen to be in good agreement with the prediction derived from packed-bed correlations of equation (12) with $A = 3^{1/2}$. It occurs when the roughness elements from opposing crack walls start to overlap.

When the crack wall separation is reduced further the friction factor falls but it does not fall nearly so far as Section 2.3 suggests. The reason may simply be that the smooth wall friction factors employed in deriving a prediction make no allowance for form drag but imperfections in the theoretical model may also be a factor.

Figure 7 gives the results for the aggregate crack. Unfortunately it was not possible to study crack separations sufficiently large to test the Nikuradse type of equation, although there is little doubt that it would be applicable. The results for the two largest crack separations of 9.85 and 19.85 mm are essentially identical and indicate that an upper limit to the friction factor is, again, achieved when the roughness elements from opposing walls start to overlap. The fully turbulent limiting friction factor is 0.2 which suggests, through equation (12), the physically unrealistic value of $A = \frac{1}{3}$ instead of the measured value of 1.46. The reason may be that the closing aggregate crack is less well represented by a packed bed than the giant's causeway and the packed-bed correlation may overestimate the form drag. Nonetheless, the arguments based upon packed beds have correctly led to the prediction of an upper limiting friction factor.

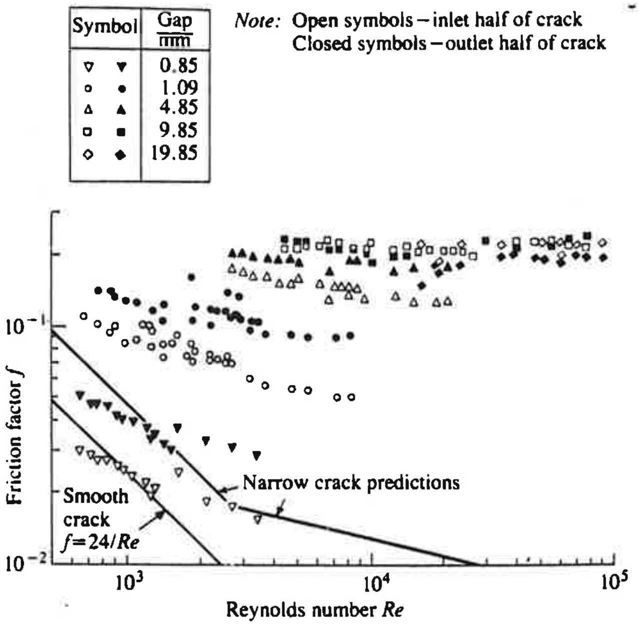

Fig. 7 Aggregate crack: friction factor versus Reynolds number

In general, Fig. 7 shows a fall in the friction factor as the crack separation decreases and it falls to about the level expected for a tortuous smooth-walled channel. This is consistent with the argument about the lack of influence of form drag given in the last paragraph. It is noted that there is a difference in the measured values of the friction factor for the two consecutive lengths of the crack in the flow direction and the difference becomes greater as the crack separation decreases. This points to a difference between the measured and the true separation, although it is noted that the test section was stripped down and reassembled without substantially affecting results. More important is that smaller crack separations than 0.85 mm could not be tested to obtain accurate results and thus make sure that the lower limiting friction factor had been achieved.

5 CONCLUSIONS

Conclusions must remain semi-quantitative since the precise morphology of crack surfaces is important. Significant conclusions about the nature of the variation of friction factor with crack wall separation are, however, achieved. Conditions as the crack wall separation reduces will be considered.

1. For wide separations the turbulent friction factor increases as predicted by a Nikuradse-type equation. The crack wall may be assumed to lie at the bottom of the roughness elements.
2. When the roughness elements from opposing surfaces of the crack start to overlap, an upper limit to the friction factor is achieved.
3. As the crack separation reduces further, the friction factor falls and may fall to a level corresponding to a smooth-walled tortuous channel.

ACKNOWLEDGEMENTS

Mr H. S. Oates gave valuable help in the design of the cracks and test sections. Mr J. Barker constructed the cracks and test sections. Both are thanked.

This work was carried out at the Central Electricity Research Laboratories and is published by permission of the Central Electricity Generating Board.

REFERENCES

1 **Nikuradse, J.** *Strömungsgesetze in rauhen Rohren*, 1933, VDI Forschungsheft 361.
2 **Button, B. L., Grogan, A. F., Chivers, T. C.** and **Manning, P. T.** Gas flow through cracks. *J. Fluids Engng*, 1978, **100**, 453–458.
3 **Bayazit, M.** Free surface flow in a channel of large relative roughness. *J. Hydraul. Res.*, 1976, **14**, 115–125.
4 **MacDonald, I. F., El-Sayed, M. S., Mow, K.** and **Dullien, F. A. L.** Flow through porous media—the Ergun equation revisited. *Ind. Engng Chem. Fundamentals*, 1979, **18**, 199–208.
5 **Ergun, S.** Fluid flow through packed columns. *Chem. Engng Prog.*, 1952, **48**, 89.
6 **Schlichting, H.** *Boundary layer theory*, 1955 (Pergamon Press, Oxford).
7 **Pfau, B.** Riffelrauhigkeit in Wandbelag von Rohrleitungen. *Verfahrenstechnik*, 1977, **11**(1), 49–52.

APPENDIX

Calculation of *A* for the giant's causeway

Figure 8 gives a plan view looking down at a corner of a cube with three faces equally inclined to the observer. The giant's causeway surface was composed of such cubes joined along the sides sloping down from the corner. We only need to study one face, which is a square with sides of length *m*. The diagonal AB in Fig. 8 is viewed without distortion. It has a length $2^{1/2}$ m, and divides the plan view into two equal triangles, which project angles of 120° at the corners of the cube. The length of the other diagonal CD is therefore $(2/3)^{1/2}$ m and the plan area of the side is $(1/3)^{1/2}$ m^2. *A* is the ratio of the true area of the side, m^2, to this plane area and is therefore $3^{1/2}$.

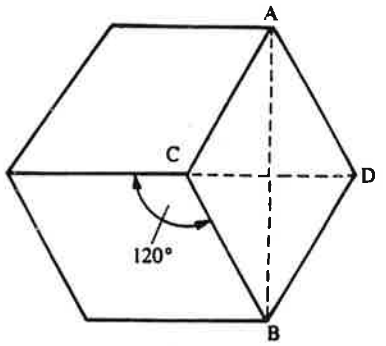

Fig. 8 Plan of roughness element of giant's causeway crack